

## Chapter VII

### CHARACTERIZATION OF DISCHARGE INSTABILITIES

#### Introduction

The investigation of nonlinear physical system exhibiting deterministically chaotic behaviour is attracting much attention. One of the interesting nonlinear systems in the context of experimental investigations is gaseous plasmas. The interest in gaseous plasmas derives from their practical applications (e.g., as medium for lasers), their potential applications (e.g., controlled fusion), or the study of their intrinsic properties, ranging from complex plasma structures up to complicated wave propagation phenomena. Discharge plasma possess a large number of degrees of freedom and is an interesting medium to test some of the universal characteristics of chaos. One of the methods to study the dynamics of nonlinear systems is by time series analysis of any measurable quantity relevant to the system. For example, in the case of discharge plasma one can monitor the discharge current to get a time series.

We have designed a discharge cell (multi electrode) to study the angular distribution of photoelectrons and hence to study the spatial variation of POG signals as they swarm through discharge

edium. In our observations, as we have changed the discharge current for different electrodes, different series of discharge instabilities were seen, with different frequencies. Details of the experimental set-up are given in the following section.

### 7.1. Experimental set-up

The schematic of the discharge cell fabricated and the experimental set-up are given in fig.7.1. The cell is a spherical glass tube provided with gas inlet and outlet ports. Desired gas (in the present case nitrogen) can be fed through a needle valve and the cell is operated as a continuous flow discharge cell by connecting the outlet to a rotary vacuum pump. Apart from the specifications for the discharge cell all other set-up for the experiment are the same as that used for POG studies described in chapter III.

To extract the relevant time series from the discharge current was monitored using the digital storage oscilloscope interfaced to a computer through its RS 232 port. Data were stored in the oscilloscope and digitized data was directly fed to the computer and saved. The digitisation of the data was carried out at suitable time interval. Fig.7.2. show some of the typical time series obtained from the present studies.

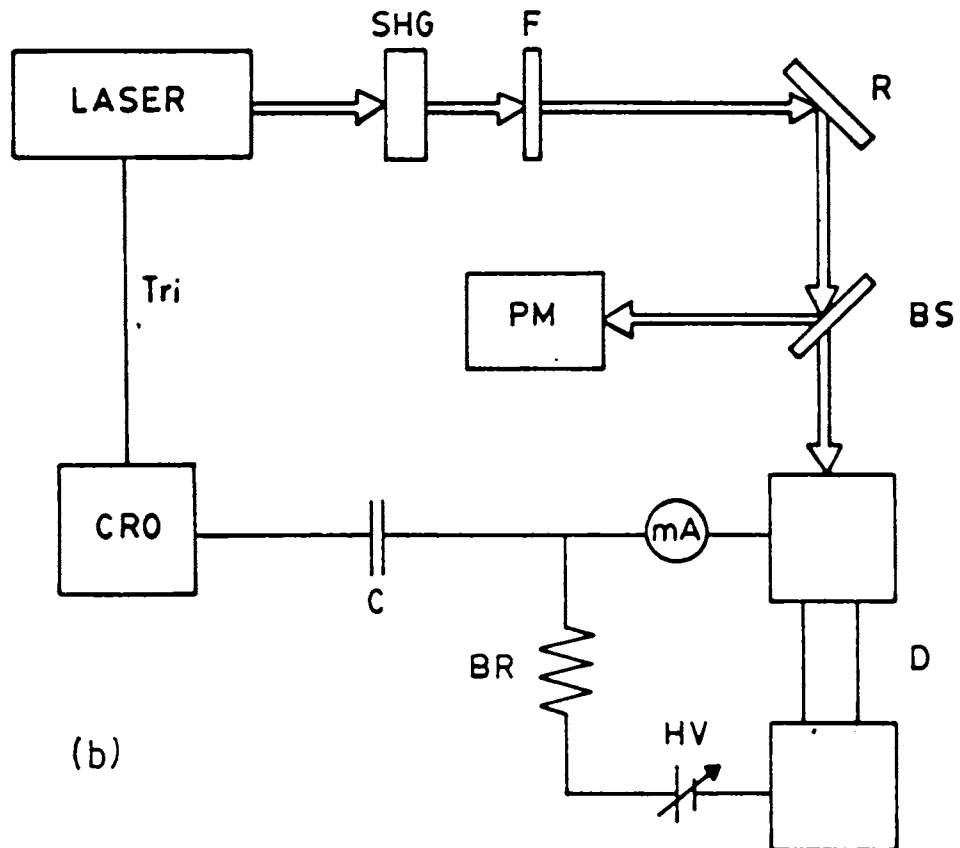
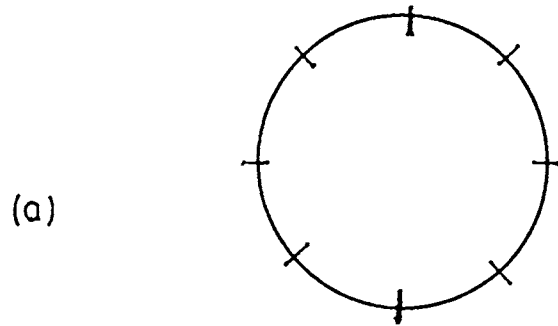
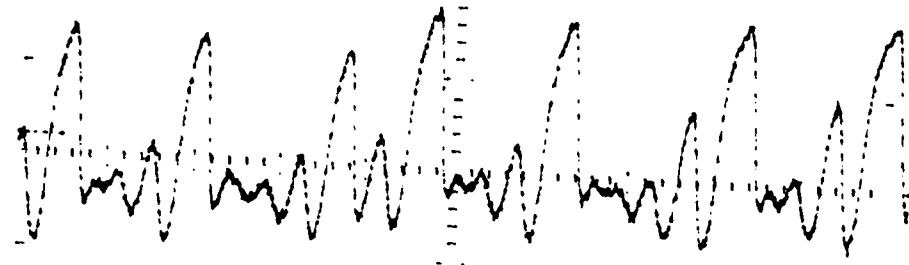
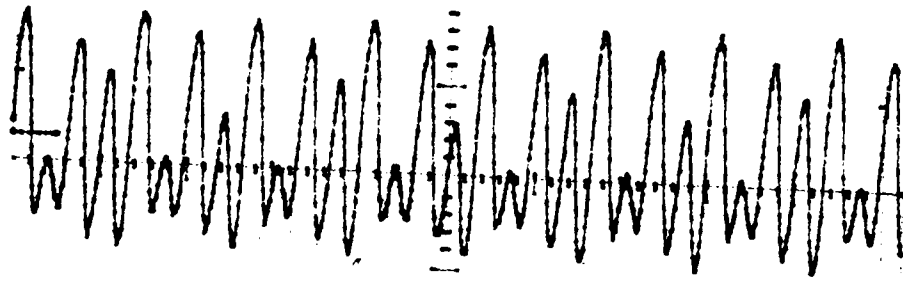


Fig.7.1 (a) Schematic of the discharge cell

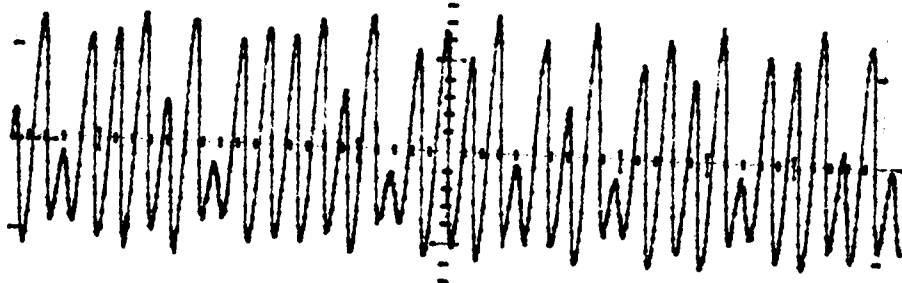
(b) Experimental set-up



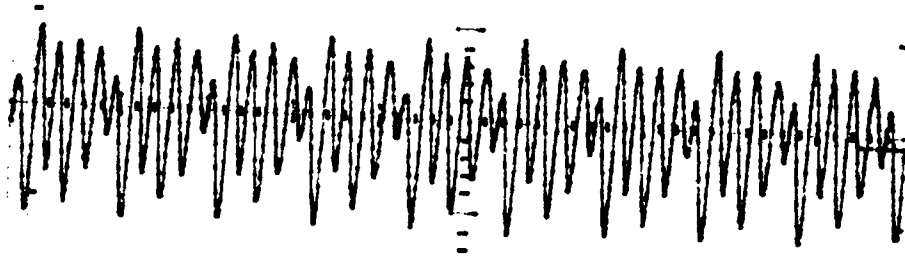
(a)



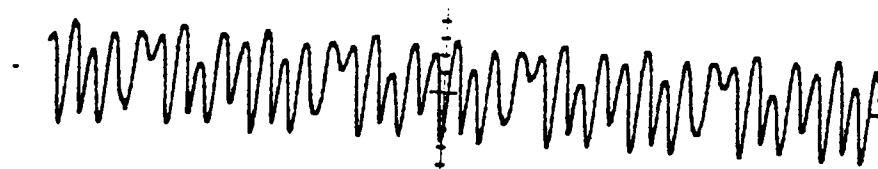
(b)



(c)



(d)



(e)

Fig.7.2 Some of the typical time series of the discharge instabilities observed.

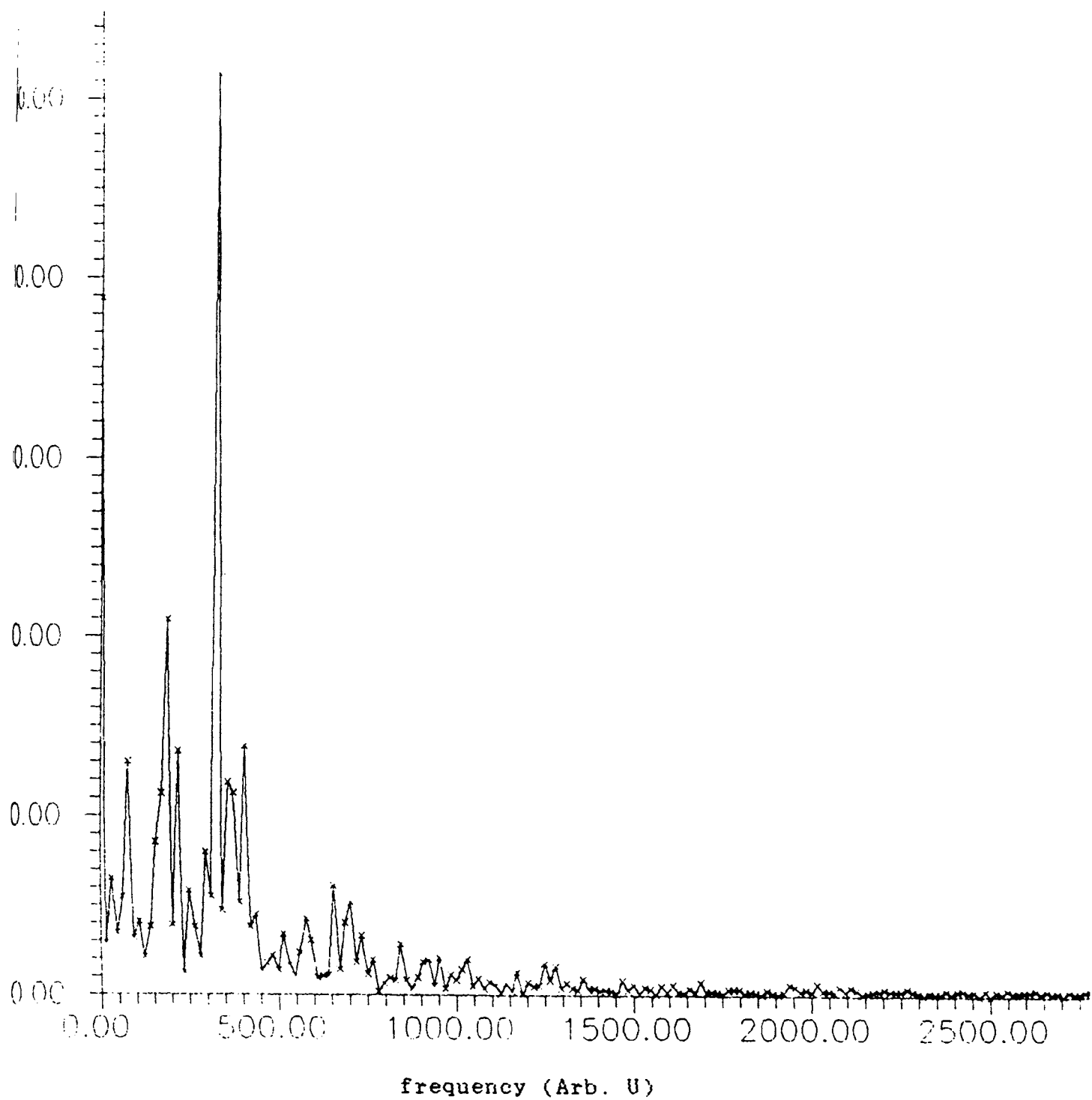


Fig.7.3 Fourier spectra of the time series 7.2e.

## 7.2. FFT and phase plot

Discrete Fourier transform is one of the usual methods used to determine the kind of evolution produced by a dynamical system by studying a time dependent signal  $\{X(t)\}$ , the time series. This will help us to find out various frequencies present in the system under consideration and enable to identify the general nature of the system. FFT is an algorithm to compute discrete Fourier transform from time series. The computed Fourier spectra of a typical time series (fig.7.2e) is given in fig.7.3. Their phase plot is also given in Figures 7.4.

## 7.3. Evaluation of $D_2$ and $K_2$ from time series - GP algorithm

Grassberger-Procaccia algorithm [1,2] is an efficient method to evaluate  $D_2$  and  $K_2$  from an experimental data obtained as a time series

$$\vec{X} = ( \vec{X}(t_1), \vec{X}(t_2), \dots, \vec{X}(t_N) )$$

where  $\vec{X}(t_i)$  is the voltage or temperature or density distribution or any fluctuation measured at the instant  $t_i$ . We usually take the time interval between two consecutive readings at constant time intervals  $\tau$ , and this series is rearranged in the following matrix form:

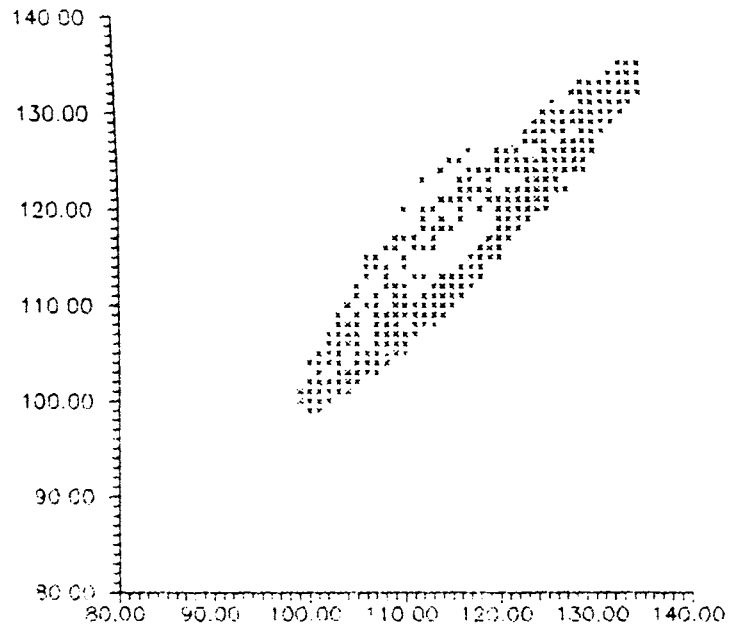


Fig.7.4 Phase plot of the time series 7.2e





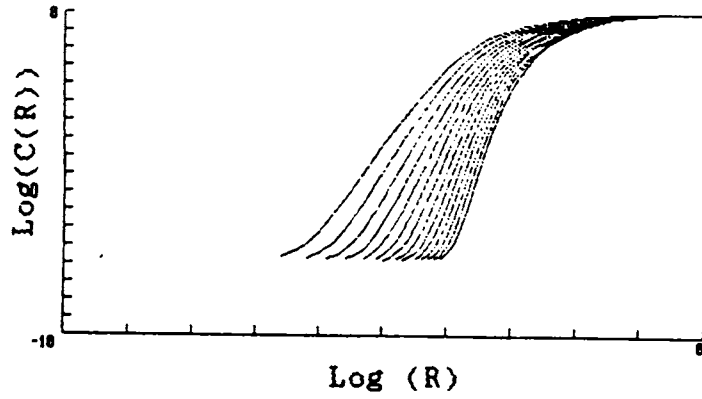


Fig.7.5 A typical plot of  $\log(C(R))$  versus  $\log(R)$ .

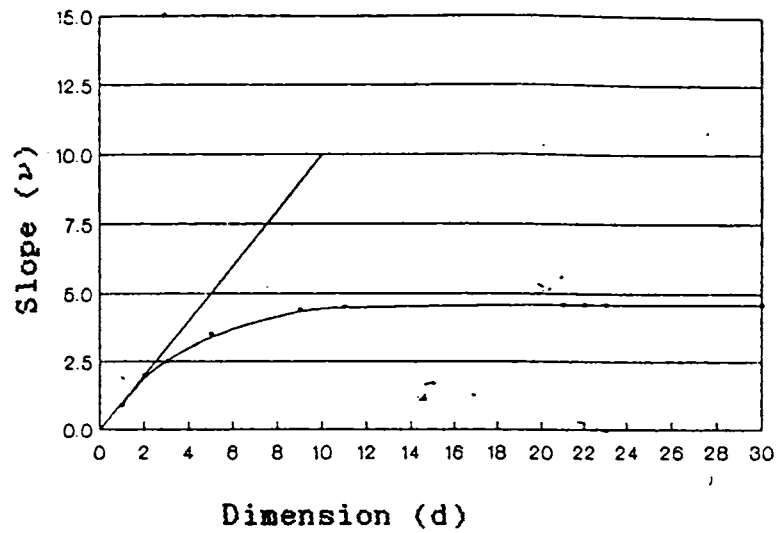


Fig.7.6 A typical plot of slope ( $\nu$ ) versus dimension ( $d$ )

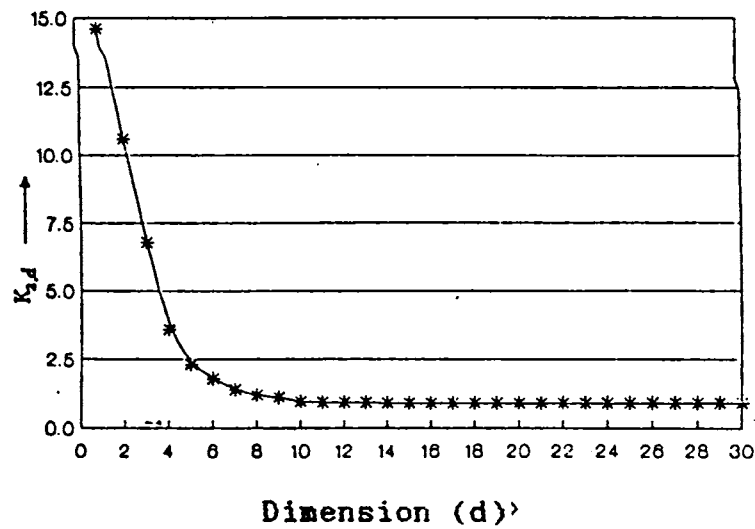


Fig.7.7 A typical plot of  $K_{2,d}$  versus dimension  $d$ .

particular dimension  $d$  of the constructed phase-space. The plot of  $\log C_d(\epsilon)$  versus  $\log(\epsilon)$  for each  $d$  (Fig.7.5) will have a linear region with a slope  $\nu$

$$\nu = \frac{\ln C_d(\epsilon)}{\ln(\epsilon)} \quad (7.4)$$

The slope  $\nu$  of the linear part of  $\log C_d(\epsilon) - \log(\epsilon)$  for each dimension  $d$  is evaluated. The plot of  $\nu$  versus  $d$  (Fig.7.6) saturates to a finite value as  $d$  increases, and the saturated value of  $\nu$  is the second order dimension or correlation dimension  $D_2$ .

The Kolmogorov second entropy  $K_2$  can be measured using the correlation integral by evaluating the ratio of spatial separation between the curves in (Fig.7.5) for dimensions  $d$  and  $(d+1)$ . The mean value of  $\frac{C_d(\epsilon)}{C_{d+1}(\epsilon)}$  over the linear range of  $\epsilon$  is calculated for each dimension and we write

$$K_{2,d} = \lim_{\substack{\epsilon \rightarrow 0 \\ \tau \rightarrow 0}} \frac{1}{\tau} \ln \left( \frac{C_d(\epsilon)}{C_{d+1}(\epsilon)} \right) \quad (7.5)$$

$K_{2,d}$  is plotted against dimension  $d$ , and the curve will saturate as shown in fig.7.7. The saturated value of  $K_{2,d}$  as  $d \rightarrow \infty$  is the second Kolmogorov entropy,

$$\lim_{d \rightarrow \infty} K_{2,d} \rightarrow K_2 \quad (7.6)$$

We can classify the system by comparing the values of  $D_2$  and  $K_2$ .  $D_2$  gives the minimum number of parameters that one requires to characterize a dissipative nonequilibrium system in its asymptotic state. As no limiting process is not involved in time, these are known as static parameters. But for  $K_2$  one takes limit of  $\tau \rightarrow 0$  or the time interval between the consecutive readings is also subjected to a limiting process.  $K_2$  is considered as a dynamic parameter and can be considered as the rate at which information about the system is lost in course of time and hence it informs how chaotic a system is.

$\log(R)$  versus  $\log(C(R))$  plot is given in fig.7.8. for the time series depicted in fig. 7.2e.  $K_2$  and  $D_2$  we reevaluated from the observed time series. It is found that  $D_2 \sim 1.2$  (fig.7.9) with a very small  $K_2$  value (fig.7.10), ( $\tau K_2 \sim 0.3$ ). Under the present experimental set-up  $D_2$  and  $K_2$  corresponding to different discharge conditions did not differ much from the above values.

#### 7.4. Evaluation of Lyapunov exponents from time series

For the nonlinear time series analysis it is of great interest to measure the Lyapunov characteristic exponents which, if positive, are the most striking evidence for chaos. Many

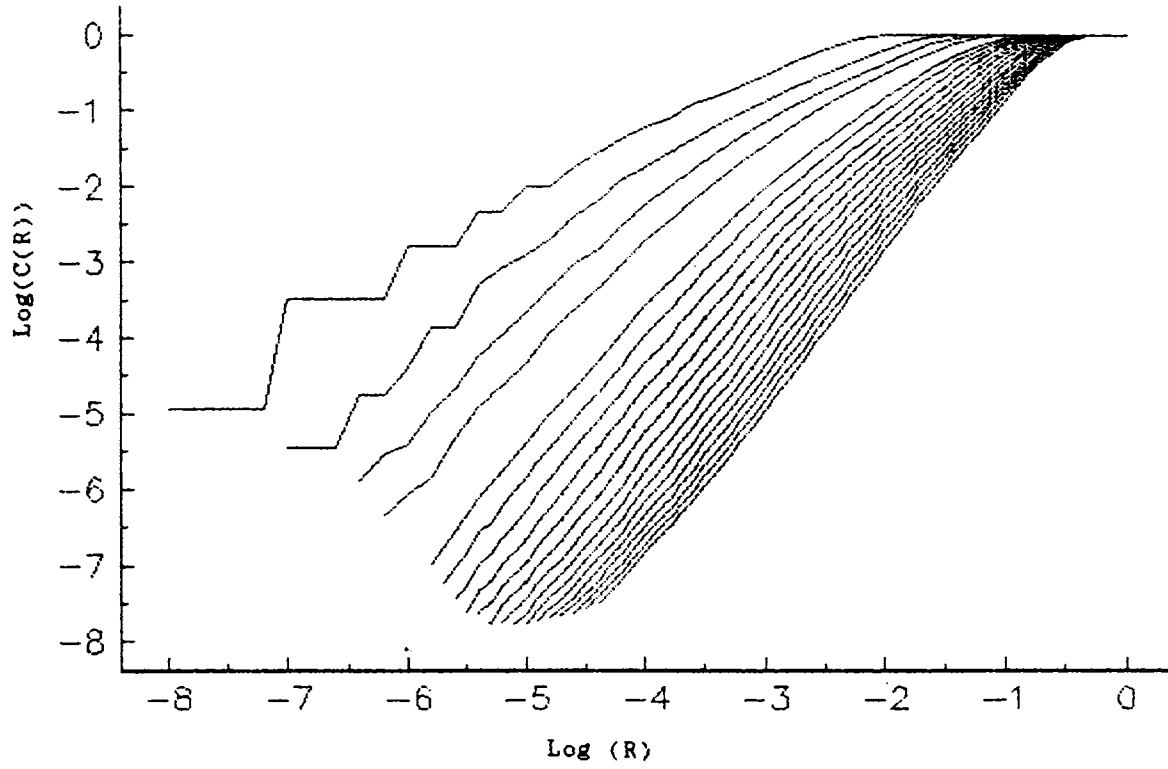


Fig.7.8  $\text{Log}(C(R))$  versus  $\text{log}(R)$  plot for the time series 7.2e.

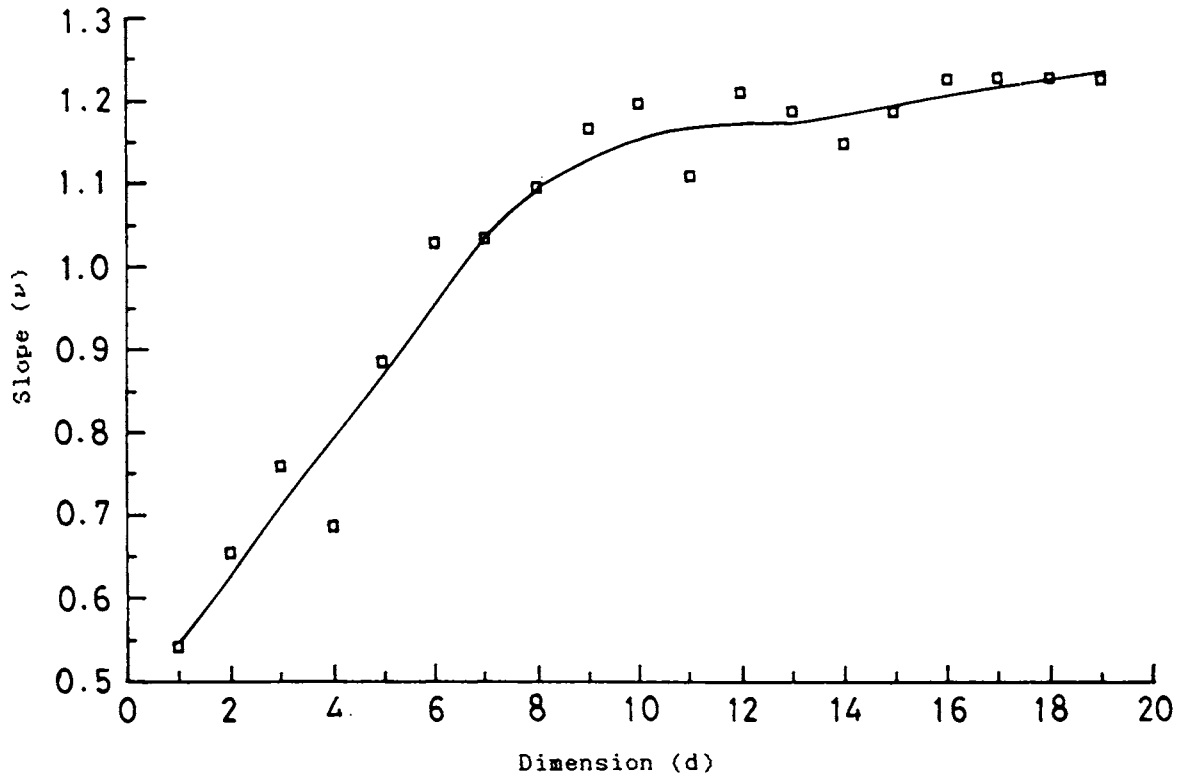


Fig.7.8 Plot of slope ( $\nu$ ) versus dimension (d) for the time series 7.2e.

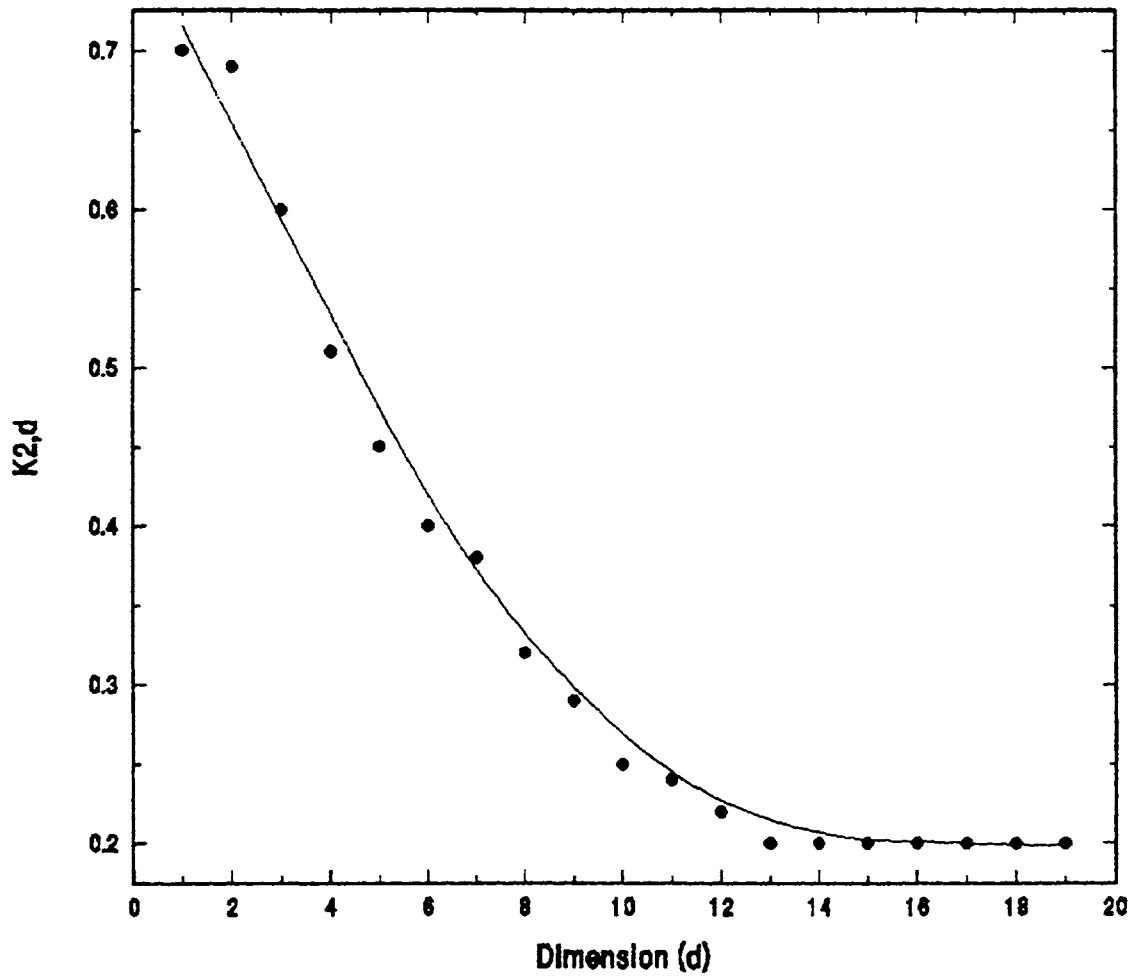


Fig.7.10 Plot of  $K_{2,d}$  versus dimension  $d$  for the time series 7.2e.

people [4-6] have devised different techniques and algorithms for the computation of Lyapunov exponents.

Practically it is not easy to tap maximum information from the time series - a univariate measurement equidistant in time, like  $\{x_t\}, t = 1, \dots, T$ . There may be defects in the data like contamination with noise or too few data etc. A univariate measurement is always a projection from the phase-space of the system where the system is deterministic to one dimensional interval of values. Hence, to reveal the properties of dynamics, a new state space has to be constructed in which the mapping from one point of the trajectory to the successive one is unique. Another difficulty is the lack of knowledge about the dynamics, which is contained only implicitly in the trajectory. One can use an algorithm which directly exploits the definition of the Lyapunov exponent in the state space to overcome such difficulties.

Here we take an algorithm to calculate maximal Lyapunov exponent proposed by Holger Kantz [7]. The basic idea of this method is that the distance between two trajectories typically increases with a rate given by the maximal Lyapunov exponent. One looks for a point of the time series which is closest to its first point. This is considered as the beginning of a neighbouring trajectory, given by the consecutive delay vectors. Then computing the distance between these two trajectories in

time. When the distance exceeds some threshold, for this point of the time series a new trajectory is searched for, when distance is as small as possible under the constraint that the new difference vector points more or less into the same direction as the old one. The logarithms of the stretching factors of the difference vectors are averaged in time to yield the maximal Lyapunov exponent.

One should be more precise in the evaluation of maximal Lyapunov exponents as the rate of increase in the neighbouring trajectories given by the maximal Lyapunov exponents is asymptotic. Because the exponential divergence of the trajectories sets in only after some transient time, since an arbitrary difference vector has to turn into the most unstable direction. Also the divergence rate of trajectories naturally fluctuates along the trajectory, with the fluctuation given by the spectrum of effective Lyapunov exponents. The maximal effective exponent ( $\lambda_\tau$ ) can be defined as

$$\lambda_\tau(t) = \lim_{\varepsilon \rightarrow 0} \frac{1}{\tau} \ln \left( \frac{|x(t+\tau) - x_\varepsilon(t+\tau)|}{\varepsilon} \right) \quad (7.7)$$

$$x(t) - x_\varepsilon(t) = \varepsilon \omega_u(t)$$

$\omega_u(t)$  is the local eigen vector associated with the maximal Lyapunov exponent  $\lambda_{\max}$ . The value for  $\lambda_\tau(t)$  depends on the



structure in tangent space and thus is position dependent. It is approximately the same for all trajectories inside a small neighbourhood. By definition the average of  $\lambda_\tau(t)$  along the trajectory is the Lyapunov exponent. Let us take an arbitrary point of the time series in an  $m$  - dimensional delay coordinates,  $x_t = (x_{t-m+1}, \dots, x_t)$ . All delay vectors of the series falling into the  $\varepsilon$ -neighbourhood  $U_t$  of  $x_t$  will be considered as the beginning of neighbouring trajectories, which are simply given by the points of the time series. If we measured the distance between neighbouring trajectories in their true phase space, we would see exactly the fluctuation of the divergence rate described by the distribution of effective Lyapunov exponents. From a time series, we could realize this situation by measuring the distance in the embedding space. But apart from the fact that we have to fix the dimension in which we search for neighbours. We do not want to distinguish any particular embedding dimension. Therefore we define the distance between a reference trajectory  $x_t$  and a neighbour  $x_i$  after the relative time  $\tau$  by

$$\text{dist}(x_t, x_i, \tau) = |x_{t+\tau} - x_{i+\tau}| \quad (7.8)$$

i.e. the modulus of the difference of the  $\tau^{\text{th}}$  scalar component of the two trajectories. These distances are projections of the difference vectors in the true phase space onto a one dimensional subspace spanned by the observable. Therefore they are modulated with  $\cos\phi$ , where  $\phi$  is the angle between the eigen vector

corresponding to  $\lambda_{\max}$  and the local direction of the subspace on which the observable lives. Like the effective Lyapunov exponent, the angle  $\phi$  depends on the position in phase space and thus is nearly the same for all neighbours  $x_i \in U_t$  of a given reference trajectory  $x_t$ , if the distance in phase space is sufficiently small.

In order to measure the maximal Lyapunov exponent we fix 't', and search for all neighbours  $x_i$  inside an  $\varepsilon$  neighbourhood  $U_t$  and compute the average of distances between all neighbouring trajectories and the reference trajectory  $x_t$  as a function of  $\tau$ .  $\tau$  is the relative time referring to the time index of the starting point. To get rid of the fluctuations we take the logarithm of these average distances, which yields the local effective Lyapunov exponent plus a fluctuation given by the angle  $\phi$ . Now this can be averaged in 't' over the full length of the time series. The local angles are averaged out and the effective exponents are averaged to the true Lyapunov exponent. Using a sophisticated algorithm for searching neighbours, this can be done very fast and is given by

$$S(t) = \frac{1}{T} \sum_{t=1}^T \ln \left\{ \frac{1}{|U_t|} \sum_{i \in U_t} \text{dist}(x, x, \tau) \right\} \quad (7.9)$$

Initially the difference vectors in the phase space are pointing in any direction, therefore the distance behaves like

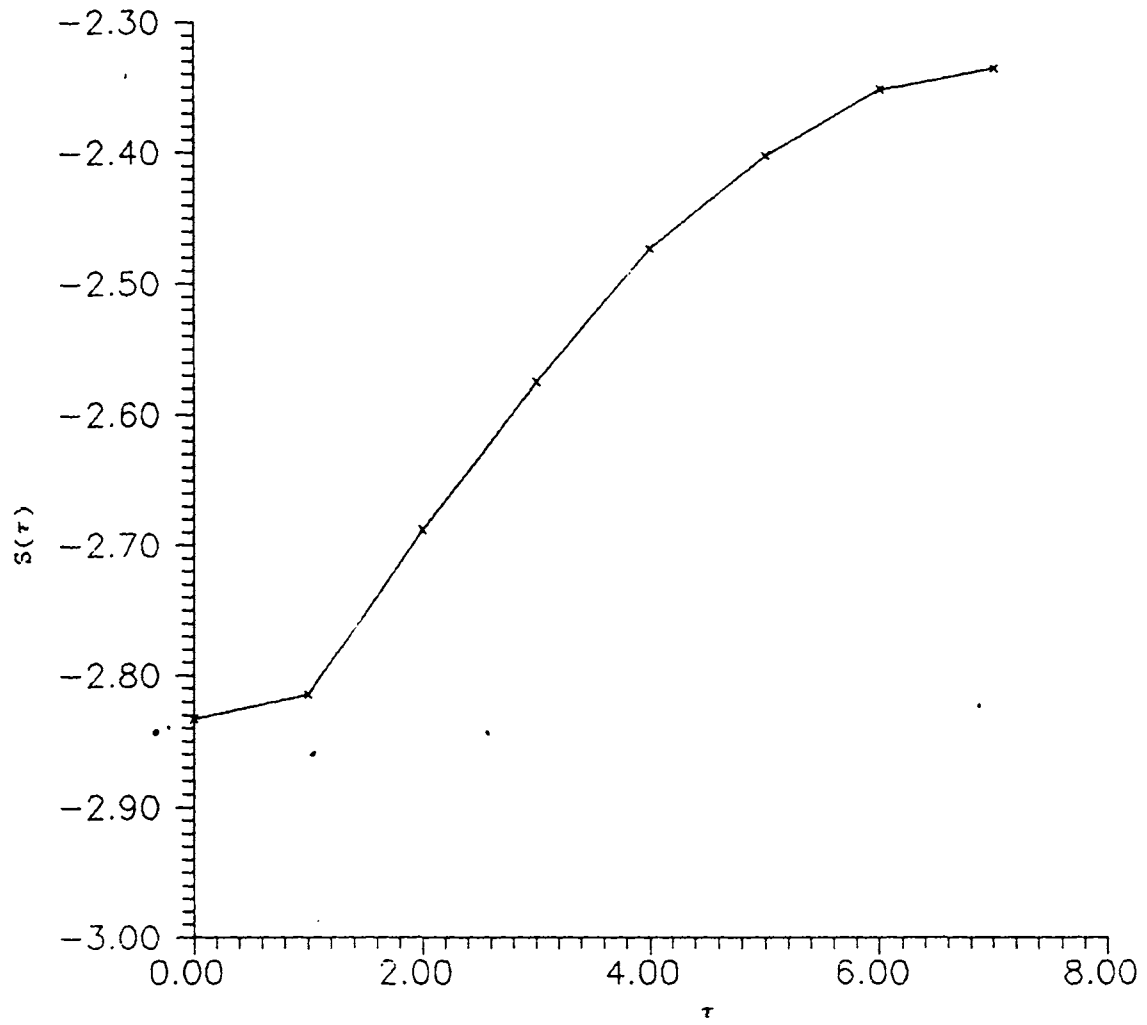


Fig.7.11 Plot of  $S(\tau)$  versus  $\tau$  for the time series 7.2e.

$$\text{dist} = \sum_i a_i \exp(\lambda_i t) \quad (7.10)$$

where  $\lambda_i$  are the effective Lyapunov exponents in the stable and unstable directions. For an intermediate range of  $\tau$ ,  $S(\tau)$  increases linearly with the slope  $\lambda$  which is the estimate of the maximal Lyapunov exponent. This is the scaling range, where on the one hand  $\tau$  is large enough such that nearly all distance vectors point into the unstable direction and on the other hand the corresponding distances  $\text{dist}(\tau)$  are smaller than the size of the attractor. When they approach the size of the attractor,  $S(\tau)$  asymptotically tends towards a constant, since the distance cannot grow more.

If the data are noisy, the typical distance between two nearby trajectories is of the order of the noise level. If we choose  $\epsilon$  smaller than the noise amplitude and if we find neighbours for this value,  $S(\tau)$  jumps from a value smaller than  $\ln \epsilon$  to a value given by the noise level at  $\tau = 1$ . If this value is not too large, one can still find a scaling range and the exponents thus found is not affected by the noise.

The numerical value for the maximal Lyapunov exponent is the slope of the curve  $S(\tau)$  in the scaling region. Lyapunov exponent was calculated for some of the selected data. A typical plot of  $S(\tau)$  versus  $\tau$  is given in fig.7.11. The slope of which is  $(0.09 \pm 0.02)$ . This small value of the Lyapunov exponent shows that the

dynamics is not in the chaotic regime. This also supports the conclusions drawn from  $K_2$  and  $D_2$  values.

The programme written to calculate the Lyapunov exponent is given in the appendix.

## References

- [1] P.Grassberger and I.Procaccia, Phys. Rev. Lett.,50,  
(1983),340
- [2] P.Grassberger and I.Procaccia, Physica D 9,(1983),189
- [3] D.S.Broomhead and G.P.King, Physica D 20,(1986),217
- [4] A.Wolf, J.B.Sniff, L.Swinney, and A.Vastano, Physica D 16,  
(1985),285
- [5] J.P.Eckman and D.Ruelle, Rev. Mod. Phys.57, (1985),617
- [6] M.Sano and Y.sawada, Phys. Rev> Lett., 55, (1985),1083
- [7] Holger Kantz,Phys. Lett. A,185,(1994),177